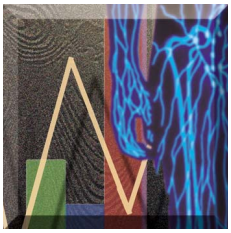

Stress Fracture Risk Analysis of the Human Femur Based on Computational Biomechanics

Liming Voo, Mehran Armand, and Michael Kleinberger

The lack of predictive tools to assess the relative risk of stress fracture injury has posed a great challenge for military readiness and competitive athletic training. This article presents a methodology of assessing such risks using computational models and biomechanical stress analysis in a human femur. Preliminary results have demonstrated the capability of our methodology in studying the effect of risk factors as independent variables, which would be very difficult, if not impossible, to accomplish by any other means. We have shown that certain geometric features are significant risk factors for femoral neck stress fracture. Further development of our methodology will enable more accurate prediction of stress fracture risk and will help in the design of optimal training regimens to minimize the risk of injury.

INTRODUCTION

Stress fracture is a type of biomechanical failure of bones caused by repetitive skeletal loads during intense physical training. Also known as fatigue fracture, it has been a well-recognized problem for athletes and military personnel. Depending on the source of the data and the method used for diagnosis, the incidence rate for stress fracture during training can range from 1 to 20%.[1–5] Aside from the obvious impact on soldiers' health, this problem imposes a significant financial burden on the military and affects our combat readiness. The incidence of stress fractures in female recruits during Army basic training is more than twice that reported for males.[1,6–8]

Stress fracture occurs mostly in the weight-bearing bones of the lower leg and foot, with fewer occurrences in the femur, pelvis, and lumbar spine.[9] Although less common than in the lower leg, stress fractures of the femoral neck (Fig. 1) are particularly serious and difficult to diagnose, requiring relatively expensive imaging modalities such as magnetic resonance imaging (MRI) and bone scans.[10–16] Delays in diagnosis can cause a fairly minor stress fracture to become a complete femoral neck fracture, which is a catastrophic event for a young soldier. Even with emergency surgery, the hip joint will often suffer from osteonecrosis, or cell death, of the femoral head as a consequence of lack of blood supply.[10–16] Such an outcome not only precludes the soldier from returning to military training but also results in a medical discharge with lifelong disability and liability.

Stress fractures of the femoral neck can be classified as compression or tension fractures. A compression stress fracture occurs at the inferior surface of the femoral neck. It is generally stable and requires only rest

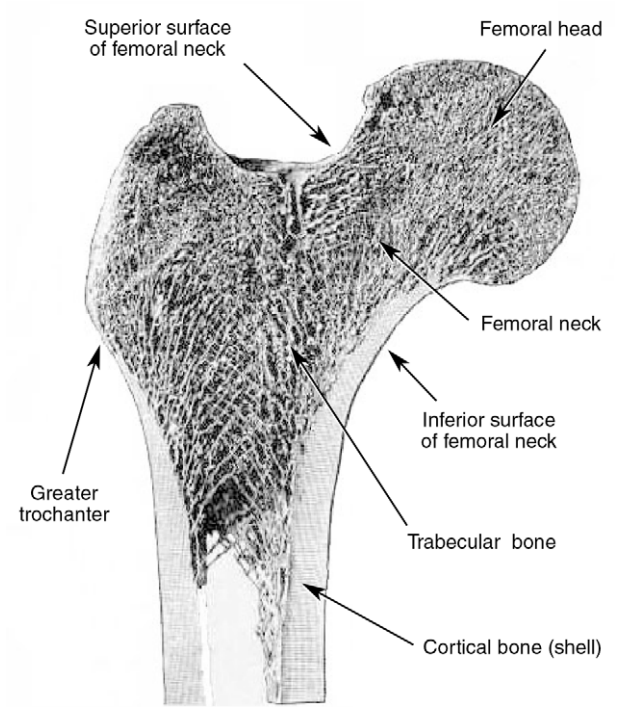

Figure 1. Anatomy of the human proximal femur (upper third of the human femur bone), which includes the femoral head, femoral neck, greater trochanter, and upper portion of the femoral stem. The femoral neck is the narrowed region directly below the femoral head. Cortical bone is the outer (hard) shell of a bone having higher material density. Trabecular bone is the relatively soft, sponge-like bone residing inside the hard cortical shell.

(no surgical intervention is needed). A tension stress fracture, on the other hand, initiates at the superior surface of the femoral neck and often progresses to a transverse fracture across the neck. It is generally unstable and requires immediate surgical intervention.[11] Identifying the risk factors in the femur of individuals who are more prone to a tension, rather than a compression, stress fracture of the femoral neck can help in the early diagnosis of this injury and prevent more catastrophic disability.

The fact that only a fraction of competitive athletes and military trainees suffer stress fractures suggests that certain people possess specific factors that increase their susceptibility. Increased susceptibility may be due to deficient material properties that fatigue more easily or to structural configurations that increase stress magnitudes.[17–19] Although the material properties of bones, such as bone density, may differ among individuals of any population, the difference would likely be smaller among competitive athletes and young military trainees. Hence it is likely that bone geometry plays a more important role in different levels of stress fracture risk in the young adult population.[20]

Numerous epidemiological and experimental studies have reported that geometric parameters, such as length and neck-shaft angle of the femoral neck, are correlated with fracture risk.[21–29] This correlation, however, has been shown to be relatively weak, probably because, in their effects on femoral bone strength, these factors are often related to each other and to other geometric parameters such as bone size. For example, a femur with a long neck is often accompanied by a bigger bone size. It is very difficult, therefore, to study the effect of these geometric factors as independent variables in a real human bone. The objective of this study is to investigate the biomechanical effects of individual geometric parameters in the femoral neck as independent variables through computational modeling and simulation using virtual bones (computer models).

MATERIALS AND METHODS

We developed a parameterized and dimensionally scalable finite element model (FEM) of a proximal human femur based on image data from computed tomography (CT). Three additional models were derived from the original model to represent variation in the three geometric parameters: cortical bone thickness in the femoral neck region, femoral neck length, and femoral neck-shaft angle (Fig. 2). Stress distributions of the four models under simulated running and jumping conditions were then analyzed to assess relative fracture risk levels.

Development of a Parameterized Finite Element Model

The proximal femur of an average male cadaver was radiographed using a CT scanner. Semi-automatic custom algorithms were applied to extract the bone's outer contours and density information from the CT image data. An elliptical fit was applied to parameterize each of the outer contours. The inner contour ellipses were calculated such that the constraint equations for cross-sectional area and mass moment of inertia along the femoral shaft and neck axes were satisfied. A three-dimensional reconstruction process was used to obtain the bone volume. Finite element mesh was then created within that volume. A parametric FEM was developed in three steps: (1) semi-automatic extraction of bone density data and outer surface geometry, (2) determination of the inner boundary of cortical bone, and (3) generation of hexahedron finite element mesh. The following paragraphs describe these three steps.

The first step was to extract density maps and bone outer-surface geometry from medical image data (CT scans, in this case). The technique of extracting bone density data from a proximal femur was adapted from the work of Oden et al.[30] A computerized algorithm cropped the CT images to include only the proximal femur. The bone density values were calculated from gray-scale values of the bone in the CT image calibrated using a combination of six phantoms having a known

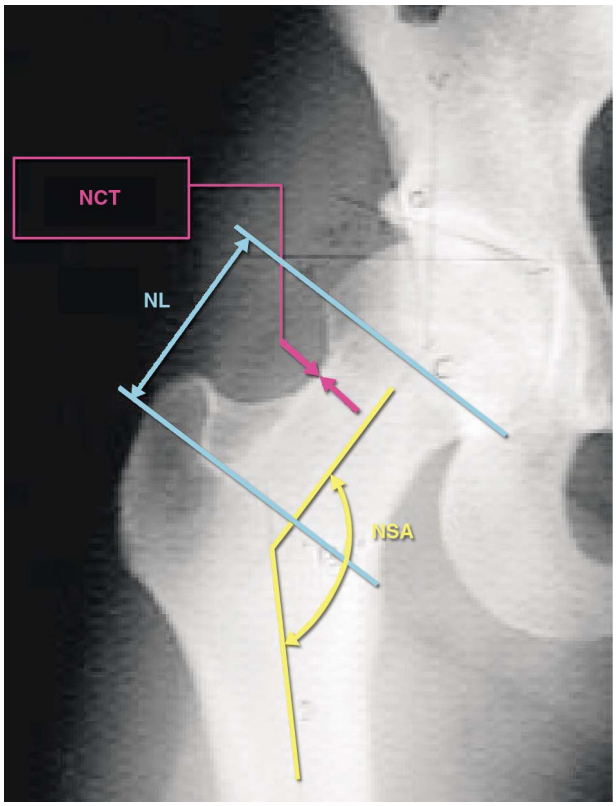

Figure 2. Three geometric variables investigated in the present study as stress fracture risk factors for the femoral neck, as marked on an X-ray image of a human hip joint (NCT = neck cortical thickness, NL = neck length, NSA = neck-shaft angle).

material density.[30] The horizontal slices were rotated such that the shaft axis was positioned vertically when looking at the longitudinal (vertical) slices of the femur. Next, the algorithm re-sliced images along the axis of the femur's shaft and neck. (The transition from shaft axis to neck axis was defined by a hyperbolic fit.) Edge extractions were performed for the outer boundaries of the femur using the re-sliced sections along the femur's neck and shaft axes. The outer boundaries of the bone cross sections were parameterized by applying a nonlinear least-squares fit of an elliptical equation.

In the second step, the inner boundaries of cortical bone were determined based on mechanical equivalence of the cross-sectional properties. The parameters of cortical/trabecular and cortical/marrow boundaries were calculated such that the cross-sectional moment of inertia (CSMI) and cross-sectional area (CSA) of the model and the original bone remained equal (both were calculated from the mass of the cross section). Density map data for each cross section plus the CSMI and CSA equations were used to calculate the appropriate elliptical fit for the cortical/trabecular or cortical/marrow boundaries. This procedure enabled us to define the inner bone geometry and its material distribution with a finite number of control points for each cross section. Applying this process to all of the bone's cross sections created a parameterized inner boundary of the proximal femur.

The algorithm accounted for the cortical thickness variations within a cross section of the bone by allowing eccentric inner contours with respect to their corresponding outer contours. Coordinates of the center of inner ellipses x_i were found by manipulating equations for the first moment of inertia as follows:

$$x_i = \frac{A_o \cdot x_o - CSA \cdot x_{cg}}{A_i}, \quad (1)$$

where x_o represents the coordinates of the outer ellipse, x_{cg} represents the coordinates of the centroid of the density map, A_o is the area under the outer elliptical ellipse, and A_i is the area under the inner ellipse.

Tissue porosity μ for the trabecular volume enclosed by the cortical bone varies with each cross section. The value of the trabecular porosity was defined and adjusted for each cross section using the following equation:

$$\mu = 1 - \frac{\sum_{j=1}^{N} d_j}{N \cdot \rho}, \quad (2)$$

where N is the number of pixels in the inner cortex, d_j is the density value for each pixel, and ρ is the average tissue density from the CT image.

For the third step, custom-designed software programs generated macros for I-DEAS software (also known as program files) that automatically generated eight-node hexahedron elements for the cortical and trabecular bone volumes. The volumes inside the inner boundaries were then filled with a hexahedron element mesh representing trabecular bone and marrow.

Computational Stress Analysis

An FEM representing the original anatomy of the proximal human femur (the Normal Model) was constructed using the methods just described. The model contains 15,360 elements with 15,633 nodes (Fig. 3). Since the model geometry was parameterized, it could readily be scaled to represent individual geometric variances in the human population. Three geometric parameters of the femoral neck were investigated in this study: cortical bone (cortex) thickness in the femoral neck region, femoral neck length, and femoral neck-shaft angle.

Three individual FEMs were created based on the original model to represent the three geometric features. To create the Thickness Model, the thickness of the superior cortical bone in the original model was reduced by 2 mm, while that of the inferior cortical bone was increased by 2 mm in the femoral neck region. A model representing a longer femoral neck (the Long-Neck

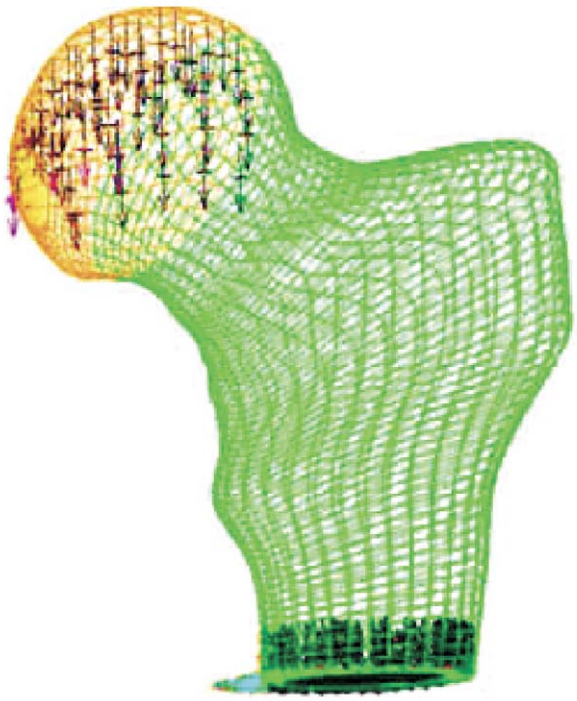

Figure 3. Finite element model of a human proximal femur with boundary and loading conditions (the Normal Model).

Model) was created by widening the distance between the adjacent cross sections in the femoral neck region with an accumulated total increase of 15 mm. To represent a smaller neck-shaft angle, the Small-Angle Model was produced by adjusting the angle between adjacent cross sections in the region that includes the greater trochanter and the femoral neck, with an accumulated total decrease of 15°.

Stress analyses were performed on all four FEMs. Material properties of the bone were assumed to be isotropic and linear elastic, and were based on similar data reported in the literature. The modulus of elasticity was 17.0 GPa for cortical bone and 1.5 GPa for trabecular bone. Poisson's ratio for the bone tissue was 0.33. Kinematic constraints were applied to the most distal part of the proximal femur. A single distributed vertical force of 2500 N was applied to the superior surface of the femoral head (Fig. 3). This loading condition was adapted to simulate the force transmitted through the hip joint when a person was in the single-leg stance phase of normal running or jumping. Stress analyses and pre- and post-processing of the models were all performed using the I-DEAS software program.

Assessment of Relative Fracture Risks

The distribution of von Mises stress in the four models was examined to compare the effects of the three geometric parameters. Peak stress values in the superior and inferior aspects of the femoral neck were then compared to the cortical bone strength reported in the literature.[31] Since the strength of human cortical bone is weaker in tension than in compression,[31] the peak von Mises stress in the superior aspect of the femoral neck (in tension) was compared with the tensile strength, while that in the inferior aspect (in compression) was compared with the compressive strength. The magnitude of peak stress relative to strength then indicated the relative risk level of bone fracture in a particular region of the femoral neck in each model. This index was used to evaluate the effect of the geometric parameters on the fracture risks of the femoral neck under such a loading condition.

RESULTS

Bone geometry did influence stress distribution in the proximal femur under the loading condition investigated (Figs. 4–7). For the Normal Model (Fig. 4), the overall maximum stress occurred at the inferior root of the femoral neck with a magnitude of 188 MPa. The peak stress in the superior aspect of the neck was approximately one-third of that in the inferior aspect. The Thickness Model (Fig. 5) had a reduced (35%) peak stress in the inferior cortex of the neck, while the stress in the superior region was essentially unchanged.

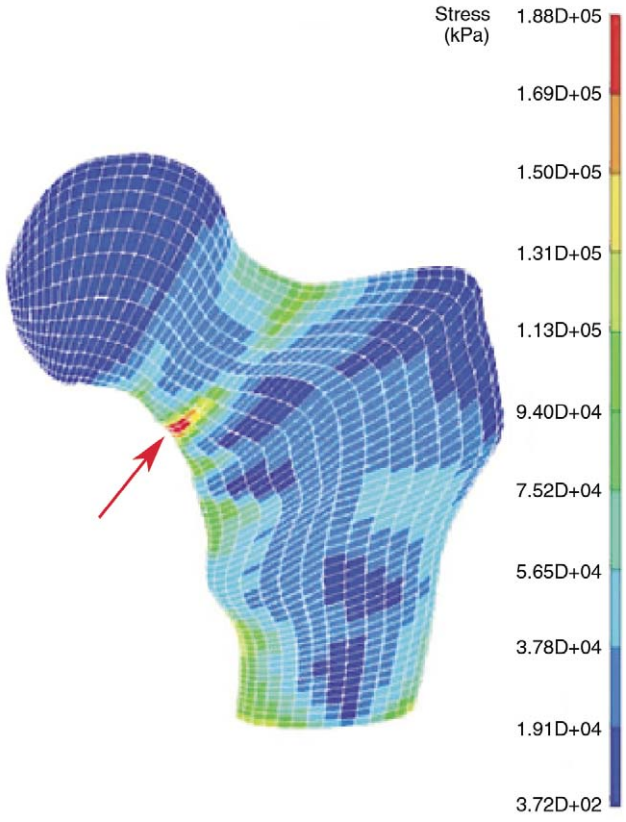

Figure 4. Distribution of von Mises stress in the Normal Model. Maximum compressive stress occurred at the inferior root of the femoral neck (indicated by the arrow).

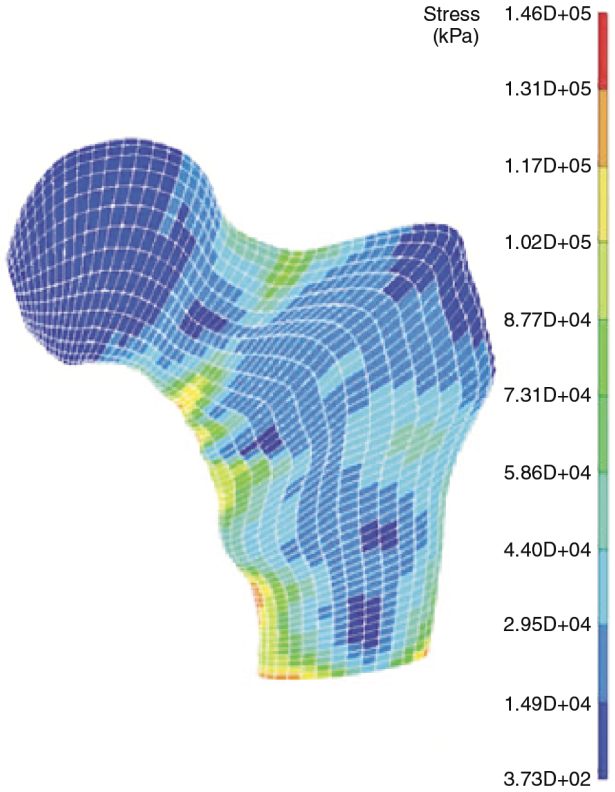

Figure 5. Distribution of von Mises stress in the Thickness Model, in which thickness in the superior aspect of the femoral neck was reduced by 50%, while that in the inferior aspect was increased by 50%.

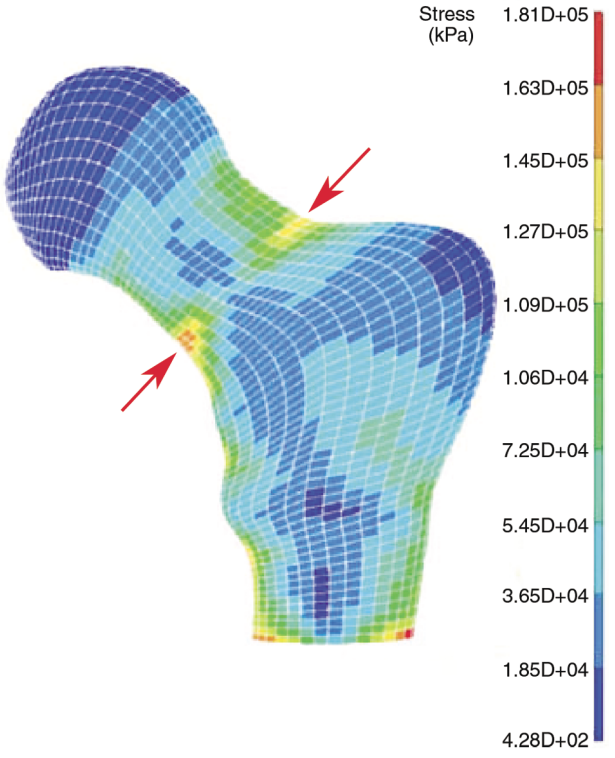

Figure 6. Distribution of von Mises stress in the Long-Neck Model, in which the femoral neck length was increased by 15 mm over that of the Normal Model.

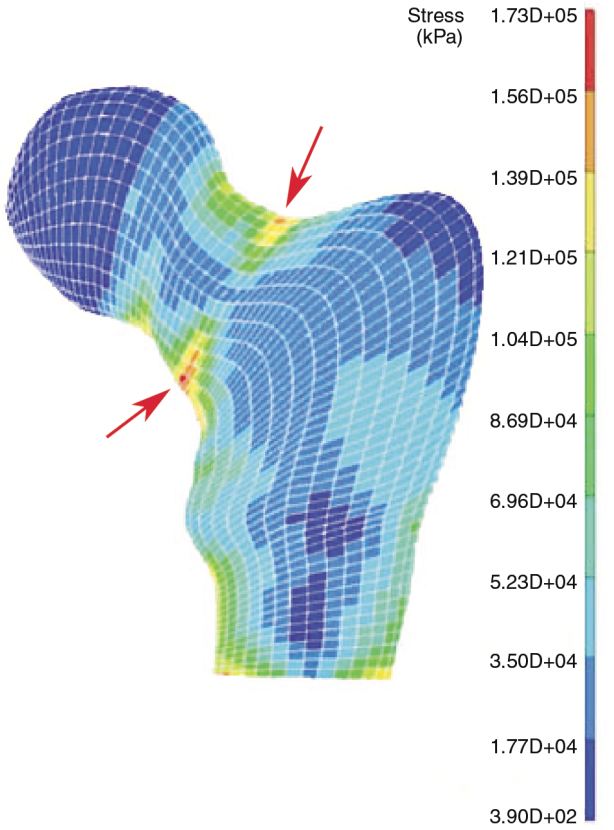

Figure 7. Distribution of von Mises stress in the Small-Angle Model, in which the femoral neck-shaft angle was reduced by 15° from that of the Normal Model.

The Long-Neck Model (Fig. 6) exhibited a significantly different stress distribution pattern compared with that of the Normal Model. The stress magnitude in the neck region was highest at the inferior root and second highest at the superior root. The peak stress in the superior neck cortex increased by approximately 65% and was only about 16% less than that in the inferior. The overall maximum stress location, however, shifted to the inferior lateral corner of the model boundary.

The Small-Angle Model (Fig. 7) had a stress distribution pattern similar to that of the Long-Neck Model. Overall maximum stress occurred at the inferior root of the neck, with a slight reduction in magnitude compared with the Normal Model (9%). However, the peak stress at the superior surface of the neck was approximately 85% higher than that in the Normal Model and was only 10% less than the overall maximum stress.

Peak stress magnitudes in the superior and inferior aspects of the femoral neck, as well as the overall maximum stress from the four models, were compared with cortical bone strength (Fig. 8). In the Normal Model, the peak stress in the inferior aspect of the neck was closest to the compressive strength of the cortical bone, while the peak stress in the superior surface of the neck was much smaller than its tensile strength. The Thickness Model had the lowest fracture risk. Both the

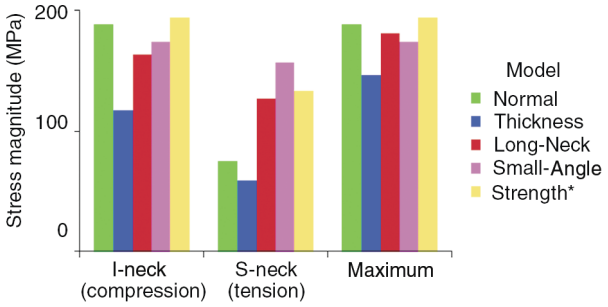

Figure 8. Comparison of peak stresses in the proximal femur with femoral cortical bone strength in compression and tension, under the loading of a 2500-N compressive force at the femoral head. (I-neck and S-neck designate inferior and superior aspects of the femoral neck; Strength* = ultimate strength of cortical bone in the human femur, from Ref. 31.)

Long-Neck Model and the Small-Angle Model had a higher risk for tension fracture in the superior neck. However, only the peak stress in the superior neck of the Small-Angle Model exceeded the tensile strength. The peak stress in the Long-Neck Model was near, but below, the tensile strength. In all the models, the overall maximum stress did not exceed the compressive strength of the cortical bone.

DISCUSSION

The present study developed four parameterized FEMs of the human proximal femur to represent its average anatomy and its variance in cortical thickness distribution, length, and angle in the femoral neck. Biomechanical stress analyses were conducted to investigate the effects of these geometric factors on relative stress fracture risks under a load condition comparable to that of running or jumping during a single-leg support phase. In the average anatomy of the proximal femur, stress concentration occurred at the inferior root of the femoral neck, where the stress mode was compressive. Reducing the cortical thickness in the superior aspect of the femoral neck by 50% and increasing it in the inferior aspect did not increase fracture risk (Fig. 8). Increasing the neck length increased the fracture risk in the superior femoral neck. Decreasing the femoral neck-shaft angle by approximately 12%, which makes the femoral neck more anatomically horizontal, resulted in a considerable increase (85%) in the magnitude of tensile stress in the superior aspects of the neck and, therefore, in fracture risk. This geometric factor would most likely be associated with a tension type of femoral neck fracture.

These results suggest that a smaller neck-shaft angle and a longer neck are significant risk factors for stress fractures of the femoral neck, particularly for the unstable type of tension fracture that initiates at the superior cortex. In a normal femur with average geometry, running and jumping produce predominantly high compressive stresses in the femoral neck area. Those minor stress fractures produced are often undetected and heal through bone remodeling without the need for medical intervention. In agreement with real cases, the results from the present study have shown that stresses in the Normal Model under running or jumping loading conditions are below the level for acute bone fracture (Fig. 8), which is measured in terms of ultimate bone strength.

A person whose bones have certain geometric features can have significantly different, and sometimes detrimental, stress reactions to the same loading conditions, as demonstrated here (Fig. 8). Note that the applied force in the present study represents the load level of a vigorous running or jumping young adult, while the ultimate strength value is derived from experimental testing of relatively older adult human specimens.[31] Nevertheless, it is reasonable to infer from results shown in Fig. 8 that young adults having a longer femoral neck and/or a smaller neck-shaft angle have a higher risk of femoral neck stress fracture, while elderly adults with such features are likely to sustain an acute femoral neck fracture when engaging in the same types of running or jumping activities.

The results of this study demonstrate that neck-shaft angle might be a very important risk factor for femoral neck stress fracture. They also indicate that a small decrease in femoral neck geometry (12% of the average angle for adults of 125°) can drastically increase (up to 85%) the stress magnitude in the critical area for unstable stress fracture. In other words, the stress in the femoral neck is very sensitive to the change in femoral neck orientation under the loading condition of jumping or running activities.

Neck-shaft angle has never been mentioned in the literature as a risk factor for stress fracture of the femur, although it has been listed as one of the risk factors for femoral neck fractures in general based on epidemiological studies.[21–29] Those studies have reported that a larger neck-shaft angle can increase the femoral neck fracture risk in an elderly population whose femoral neck fractures mostly resulted from an impact load to their greater trochanter during a fall from a standing position.[21,22,24–27] Our computational study using numerical models provides further biomechanical validation that neck-shaft angle is a risk factor for femoral neck fracture under a variety of loading conditions. These results also provide a quantitative sensitivity analysis of this geometric factor in its influence on the fracture risk of the femoral neck. The results also suggest that the neck-shaft angle could be a key variable in determining whether the fracture outcome is the stable compressive type or the unstable tension type in the femoral neck under such loading conditions.

A femur with a longer neck may be at a higher risk for the tension type of fracture compared with a similar-sized femur with an average neck. The influence of

femoral neck length is more difficult to determine because a longer neck in the human femur is often associated with larger bone size, a factor known to be correlated with a reduction in fracture risk in the femoral neck.[21–29] This may be partially responsible for the lack of statistical significance in some reported results and even conflicting findings in others. Such confounding effects were avoided in the present computational study by keeping all other factors constant in a virtual human anatomic specimen, a condition very difficult to obtain in a real human anatomic specimen. Like the influence of the neck-shaft angle, but to a lesser extent, neck length tends to increase the risk of fracture caused by tensile stress while tending to reduce the risk of fracture caused by compressive stress (Fig. 8). The fact that previous epidemiological studies[21–29] did not separate the compressive and tension type of femoral neck fractures might have also reduced the power of their statistical analyses. Such statistical power could be increased if the tension fracture and compression fracture cases were separated into two sample groups.

The present study did not include the muscle loads to the bone. Previous studies have suggested that muscle fatigue is likely to increase the risk of stress fracture.[4,7] A fatigued muscle has reduced ability to exert force in the bone. With less muscle force, stress patterns in the bone under the same physical activities would certainly be altered. In the proximal femur, the tensile force from muscles attached to the greater trochanter may change the location and magnitude of the stress concentration. By omitting the muscle force in the model simulation, the present study assumes a worst-case scenario, when the muscles attached to the greater trochanter are completely fatigued and unable to exert any force. Including muscle action in the computational simulation would significantly expand the application of our models to investigate the effects of fatigue and help to determine optimal training regimens based on fitness levels.

This computational study did not include the process of bone remodeling. Like fatigue fractures in engineering materials, stress fracture damage in bones starts at the submicroscopic level, grows to microscopic cracks, and progresses to macroscopic fracture. Unlike engineering materials, though, bone tissue can heal itself at every stage of damage as a result of biological remodeling processes. Including such biological processes would expand the present method into the time domain and significantly improve its power in predicting stress fracture risks. It would again help to design an optimal training regimen where stress fracture risk is kept at a minimum.

Another limitation of the current study is that the cross-sectional geometry of the models is approximated by a series of ellipses such that the CSA and area moment of the model and the real bone are equal. Although the model geometry is derived from CT images of a real human femur, the approximation technique used here may have significantly altered the absolute thickness of the cortical shell and, hence, the absolute magnitude of the stress in response to loading. Therefore, the absolute stress magnitudes in the present study are not expected to be accurate. Since the primary objective here was to investigate the relative effects of geometric factors, the stress magnitude in one location relative to another location is still valid. Nevertheless, results reported in this article should be considered preliminary. Work is under way to develop a new technique that would more accurately represent the cross-sectional geometry of the bone.

CONCLUSION

We have developed a computational method to investigate three individual geometric factors as independent variables that may correlate with stress fracture risk to the human femoral neck. Our results have shown that both femoral neck length and neck-shaft angle affect the biomechanical risk of femoral neck stress fracture. A smaller femoral neck-shaft angle not only can increase the risk for femoral neck stress fracture but also is a key risk factor for the unstable tension type of fracture. Although the present results are preliminary, they demonstrate the power and flexibility of computational modeling and simulation in the biomechanical assessment of bone stress fracture risks. With improved geometric accuracy, our future computational models can potentially be used to more quantitatively determine the contribution of individual biomechanical factors and their combination in fracture risk prediction. Recommended further work includes adding bone remodeling processes and muscle function to the computational simulation, which will enable a more accurate biomechanical prediction of stress fracture injury risks and help in the design of an optimal training regimen that keeps stress fracture risk to a minimum.

REFERENCES

[1]Deuster, P. A., Jones, B. H., and Moore, J., "Patterns and Risk Factors for Exercise-Related Injuries in Women: A Military Perspective," *Mil. Med.* **162**, 649–655 (1997).

[2]Givon, U., Friedman, E., Reiner, A., Vered, I., Finestone, A., and Shemer, J., "Stress Fractures in the Israeli Defense Forces from 1995 to 1996," *Clin. Orthop.* **373**, 227–232 (2000).

[3]Jordan, G., and Schwellnus, M. P., "The Incidence of Overuse Injuries in Military Recruits During Basic Military Training," *Mil. Med.* **159,** 421–426 (1994).

[4]Jones, B. H., and Knapik, J. J., "Physical Training and Exercise-Related Injuries. Surveillance, Research and Injury Prevention in Military Populations," *Sports Med.* **27**, 111–125 (1999).

[5]Milgrom, C., Giladi, M., Stein, M., Kashtan, H., Margulies, J. Y., et al., "Stress Fractures in Military Recruits. A Prospective Study Showing an Unusually High Incidence," *J. Bone Joint Surg. Br.* **67**, 732–735 (1985).

[6]Brudvig, T. J. S., Gudger, T. D., and Obermeyer, L., "Stress Fractures in 285 Trainees: A One-Year Study of Incidence as Related to Age, Sex, and Race," *Mil. Med.* **148**, 666–667 (1983).

[7]Friedl, K. E., Nuovo, J. A., Patience, T. H., and Dettori, J. R., "Factors Associated with Stress Fracture in Young Army Women: Indications for Further Research," *Mil. Med.* **157**, 334–338 (1992).

[8]Milgrom, C., Finestone, A., Shlamkovitch, N., Rand, N., Lev, B., et al., "Youth Is a Risk Factor for Stress Fracture: A Study of 783 Infantry Recruits," *J. Bone Joint Surg.* **76B**, 20–22 (1994).
[9]Bennell, K. L., and Brukner, P. D., "Epidemiology and Site Specificity of Stress Fractures," *Clin. Sports Med.* **16**, 179–196 (1997).
[10]Boden, B. P., and Speer, K. P., "Femoral Stress Fractures," *Clin. Sports Med.* **16**, 307–317 (1997).
[11]Boden, B. P., and Osbahr, D. C., "High-Risk Stress Fractures: Evaluation and Treatment," *J. Am. Acad. Orthop. Surg.* **8**, 344–353 (2000).
[12]Clough, T. M., "Femoral Neck Stress Fracture: The Importance of Clinical Suspicion and Early Review," *Br. J. Sports Med.* **36**, 308–309 (2002).
[13]Egol, K. A., Koval, K. J., Kummer, F., and Frankel, V. H., "Stress Fractures of the Femoral Neck," *Clin. Orthop.* **34**, 72–78 (1998).
[14]Johansson, C., Ekenman, I., Tornkvist, H., and Eriksson, E., "Stress Fractures of the Femoral Neck in Athletes: The Consequence of a Delay in Diagnosis," *Am. J. Sports Med.* **18**, 524–528 (1990).
[15]Muldoon, M. P., Padgett, D. E., Sweet, D. E., Deuster, P. A., and Mack, G. R., "Femoral Neck Stress Fractures and Metabolic Bone Disease," *J. Orthop. Trauma* **15**, 181–185 (2001).
[16]Volpin, G., Hoerer, D., Groisman, G., Zaltzman, S., and Stein, H., "Stress Fractures of the Femoral Neck Following Strenuous Activity," *J. Orthop. Trauma* **4**, 394–398 (1990).
[17]Myburgh, K. H., Hutchins, J., Fataar, A. B., Hough, S. F., and Noakes, T. D., "Low Bone Density Is an Etiologic Factor for Stress Fractures in Athletes," *Ann. Intern. Med.* **113**, 754–759 (1990).
[18]Nakamura, T., Turner, C. H., Yoshikawa, T., Slemenda, C. W., Peacock, M., et al., "Do Variations in Hip Geometry Explain Differences in Hip Fracture Risk Between Japanese and White Americans?" *J. Bone Miner. Res.* **9**, 1071–1076 (1994).
[19]Nelson, D. A., Jacobsen, G., Barondess, D. A., and Parfitt, A. M., "Ethnic Differences in Regional Bone Density, Hip Axis Length, and Lifestyle Variables Among Healthy Black and White Men," *J. Bone Miner. Res.* **10**, 782–787 (1995).
[20]Beck, T. J., Ruff, C. B., Shaffer, R. A., Betsinger, K., Trone, D. W., and Brodine, S. K., "Stress Fracture in Military Recruits: Gender Differences in Muscle and Bone Susceptibility Factors," *Bone* **27**, 437–444 (2000).
[21]Alonso, C. G., Curiel, M. D., Carranza, F. H., Cano, R. P., and Perez, A. D., "Femoral Bone Mineral Density, Neck Shaft Angle and Mean Femoral Neck Width as Predictors of Hip Fracture in Men and Women," *Osteoporos. Int.* **11**, 714–720 (2000).
[22]Bergot, C., Bousson, V., Meunier, A., Laval-Jeantet, M., and Laredo, J. D., "Hip Fracture Risk and Proximal Femur Geometry from DXA Scans," *Osteoporos. Int.* **13**, 542–550 (2002).
[23]Cheng, X. G., Lowet, G., Boonen, S., Nicholson, P. H. F., Brys, P., et al., "Assessment of the Strength of Proximal Femur *in vitro*: Relationship to Femoral Bone Mineral Density and Femoral Geometry," *Bone* **20**, 213–218 (1997).
[24]Faulkner, K. G., Cummings, S. R., Black, D., Palermo, L., Gluer, C. C., and Genant, H. K., "Simple Measurement of Femoral Geometry Predicts Hip Fracture: The Study of Osteoporotic Fractures," *J. Bone Miner. Res.* **8**, 1211–1217 (1993).
[25]Gnudi, S., Ripamonti, C., Gualitieri, G., and Malavolta, N., "Geometry of Proximal Femur in the Prediction of Hip Fracture in Osteoporotic Women," *Br. J. Radiol.* **72**, 729–733 (1999).
[26]Gnudi, S., Ripamonti, C., Lisi, L., Fini, M., Giardino, R., and Giavaresi, G., "Proximal Femur Geometry to Detect and Distinguish Femoral Neck Fractures from Trachanteric Fractures in Postmenopausal Women," *Osteoporos. Int.* **13**, 69–73 (2002).
[27]Karlsson, K. M., Sernbo, I., Obrant, K. J., Redlund-Johnell, I., and Johnell, O., "Femoral Neck Geometry and Radiographic Signs of Osteoporosis as Predictors of Hip Fractures," *Bone* **18**, 327–330 (1996).
[28]Kukla, C., Gaebler, C., Pichl, R. W., Prokesch, R., Heinze, G., and Heinz, T., "Predictive Geometric Factors in a Standardized Model of Femoral Neck Fracture: Experimental Study of Cadaveric Human Femurs," *Int. J. Care Injured* **33**, 427–433 (2002).
[29]Pinilla, T. P., Boardman, K. C., Bauxsein, M. L., Myers, E. R., and Hayes, W. C., "Impact Direction from a Fall Influences the Failure Load of the Proximal Femur as Much as Age-Related Bone Loss," *Calcif. Tissue Int.* **58**, 231–235 (1996).
[30]Oden, Z. M., Selvitelli, D. M., and Bouxsein, M. L., "Effect of Local Density Changes on the Failure Load of the Proximal Femur," *J. Orthop. Res.* **17**, 661–667 (1999).
[31]Reilly, D. T., and Burstein, A. H., "The Elastic and Ultimate Properties of Compact Bone Tissue," *J. Biomech.* **8**, 393–405 (1975).

ACKNOWLEDGMENT: This work was supported in part by the Independent Research and Development Grant in Biomedicine from APL and a grant from the U.S. Army Medical Research and Materiel Command (award number DAMD17-03-0711).

THE AUTHORS

The Stress Fracture Biomechanics (SFBM) Team is led by **Liming Voo**, the project Principal Investigator (PI). Dr. Voo is a Senior Research Scientist in APL's National Security Technology Department (NSTD) and a part-time Associate Research Professor in the JHU Whiting School of Engineering. A Ph.D. in biomedical and mechanical engineering, Dr. Voo has collaborated with orthopedic and neurological surgeons on the biomechanics of impact, injury, and surgery for over 15 years. His expertise is in injury risk assessment, computational analysis, and experimental testing of biological structures and systems. **Mehran Armand** is a Senior Professional Staff member in NSTD and an adjunct faculty member at the Catholic University of America. A Ph.D. in mechanical engineering and kinesiology, Dr. Armand serves as co-PI of the project and leads the modeling efforts with his expertise in orthopedic biomechanics and computational modeling. **Michael Kleinberger** is an APL Principal Professional Staff member and an adjunct faculty member in the JHU Bloomberg School of Public Health. At APL, Dr. Kleinberger is Supervisor of the Applied Chemical and Biological Sciences Group and Program Manager for Biomechanics and Injury Science under the Biomedical Business Area. A Ph.D. in biomedical engineering, he provides expertise in injury mechanisms and impact biomechanics, with previous experience in developing safety standards at the National Highway Traffic Safety Administration. The SFBM Team can be contacted through the PI, Dr. Voo. His e-mail address is liming.voo@jhuapl.edu.


Liming Voo


Mehran Armand


Michael Kleinberger